

Leading superconducting instabilities in three-dimensional models for Sr_2RuO_4

Astrid T. Rømer,¹ T. A. Maier,² Andreas Kreisel,³ P. J. Hirschfeld,⁴ and Brian M. Andersen¹

¹*Niels Bohr Institute, University of Copenhagen, 2100 Copenhagen, Denmark*

²*Center for Nanophase Materials Sciences, Oak Ridge National Laboratory, Oak Ridge, Tennessee 37831, USA*

³*Institut für Theoretische Physik, Universität Leipzig, D-04103 Leipzig, Germany*

⁴*Department of Physics, University of Florida, Gainesville, Florida 32611, USA*

(Dated: April 7, 2022)

The unconventional superconductor Sr_2RuO_4 has been the subject of enormous interest over more than two decades, but until now the form of its order parameter has not been explicitly determined. Since groundbreaking NMR experiments revealed recently that the pairs are of dominant spin-singlet character, attention has focused on time-reversal symmetry breaking linear combinations of s -, d - and g -wave one-dimensional (1D) irreducible representations. However, a state of the form $d_{xz} + id_{yz}$ corresponding to the two-dimensional representation E_g has also been proposed based on some experiments. We present a systematic study of the stability of various superconducting candidate states, assuming that pairing is driven by the fluctuation exchange mechanism, including a realistic three-dimensional Fermi surface, full treatment of both local and non-local spin-orbit couplings, and a wide range of Hubbard-Kanamori interaction parameters U, J, U', J' . The leading superconducting instabilities are found to exhibit nodal even-parity $A_{1g}(s')$ or $B_{1g}(d_{x^2-y^2})$ symmetries, similar to the findings in two-dimensional models without longer-range Coulomb interaction which tends to favor d_{xy} over $d_{x^2-y^2}$. Within the so-called Hund's coupling mean-field pairing scenario, the $E_g(d_{xz}/d_{yz})$ solution can be stabilized for large J and specific forms of the spin-orbit coupling, but for all cases studied here the eigenvalues of other superconducting solutions are significantly larger when the full fluctuation exchange vertex is included in the pairing kernel. Additionally, we compute the spin susceptibility in relevant superconducting candidate phases and compare to recent neutron scattering and NMR Knight shift measurements. It is found that $d_{xz} + id_{yz}$ order supports a neutron resonance in its superconducting phase, in contrast to a recent experiment [K. Jenni *et al.*, Phys. Rev. B **103**, 104511 (2021)], whereas $s' + id_{x^2-y^2}$ does not. Furthermore, comparison of the Knight shift reveals that $s' + id_{x^2-y^2}$ exhibits a larger low-temperature shift than $d_{xz} + id_{yz}$.

I. INTRODUCTION

The superconducting state of Sr_2RuO_4 remains unresolved and after nearly three decades of study, the current lack of consensus on the nature of the superconducting ground state highlights the need for better quantitative theoretical descriptions of unconventional superconductivity [1]. There is consensus on some qualitative aspects: for example, recent ultrasound experiments impose important constraints on the possibilities of superconducting orders in Sr_2RuO_4 , suggesting composite pairing solutions where the product of two distinct superconducting components transforms as $B_{2g}(d_{xy})$ [2, 3]. In two-dimensional (2D) models, this leaves open the possibility of nearly degenerate superconducting instabilities belonging to different irreducible representations forming solutions of the form $d_{x^2-y^2} + ig_{(x^2-y^2)xy}$ [4, 5] or $s' + id_{xy}$ [6, 7]. (We denote by s' (s) order parameters with nodal (nodeless) A_{1g} symmetry.) The 2D representation $E_u : p_x/p_y$ seems ruled out due to a pronounced drop in Knight shift observed by nuclear magnetic resonance (NMR) [8–10]. However, as pointed out recently, when considering the third spatial dimension there exists another 2D irreducible representation of the D_{4h} point group which could potentially encompass the observations from NMR, ultrasound experiments and μSR , namely the even-parity solution $E_g : d_{xz}/d_{yz}$ [2, 8, 11, 12]. This state, however, ex-

hibits a controversial nodal structure with (horizontal) line nodes at $k_z = 0$ [13], and relies on interlayer Cooper pairing despite the pronounced 2D electronic structure of Sr_2RuO_4 .

Most previous theoretical works addressing the gap structure of Sr_2RuO_4 were restricted to the two spatial dimensions of the RuO_2 planes. This approximation appears natural based on the pronounced 2D structure of the system as observed by e.g. the resistivity anisotropy ratio [16], de Hass-van Alphen oscillations [17], and angular resolved photoemission spectroscopy (ARPES) [18–20]. However, the fact that the orbital content at the Fermi surface varies along k_z as a result of spin-orbit coupling (SOC) [21] makes this state more plausible. Recently, the importance of the third dimension on the nature of the superconducting state was explored in Refs. 6, 22–26. In particular, local pairing originating from large Hund's couplings treated within mean-field theory can stabilize spin-triplet, orbital-singlet superconductivity [14, 27], which despite the spin-triplet structure can be compatible with a Knight shift reduction [22, 23, 28, 29].

When onsite attractive interactions arise from large Hund's coupling, the superconducting gap structure is inherited from the normal state band structure. This gives rise to an inter-orbital spin-triplet pairing gap if onsite SOC dominates [14, 30]. However, other solutions can materialize in the presence of sizable momentum-dependent spin-orbit couplings (k-SOC). For example,

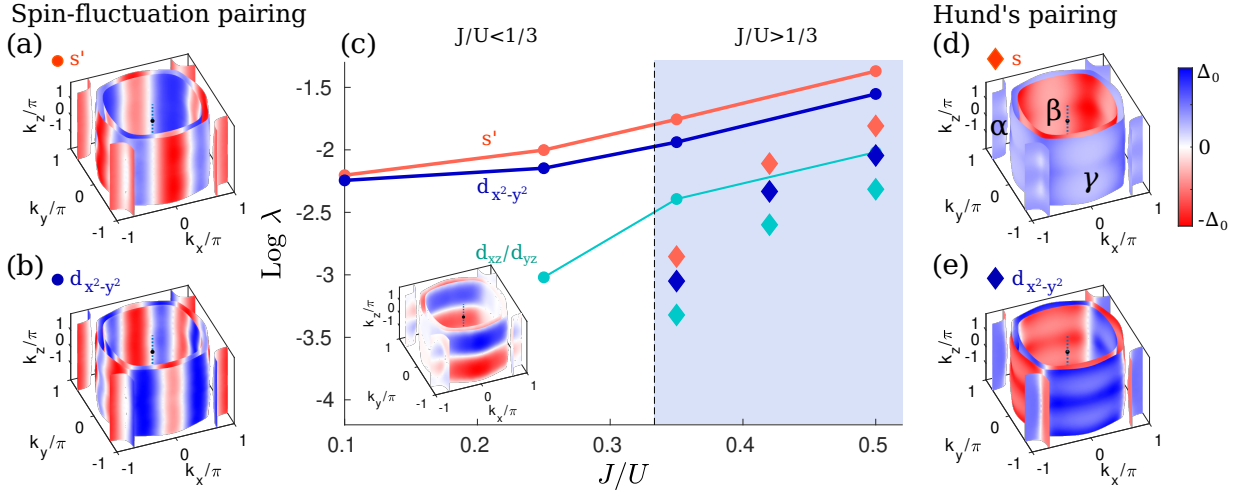


FIG. 1. (a,b) Leading nodal s' and subleading $d_{x^2-y^2}$ gap structures arising within spin-fluctuation mediated pairing for $U = 100$ meV and $J/U = 0.25$. (c) Evolution of the eigenvalues of the linearized gap equation [Eq. (17)] as a function of Hund's coupling for onsite Coulomb repulsion $U = 100$ meV. Note the logarithmic scale. The orange (blue) line displays the eigenvalue of the s' ($d_{x^2-y^2}$) solutions, while the turquoise line shows the eigenvalue of the d_{xz}/d_{yz} solution, all obtained within the spin-fluctuation mediated pairing scenario. Diamond symbols display the eigenvalues of the local Hund's coupling pairing scenario with s shown by orange, $d_{x^2-y^2}$ shown by blue diamonds and d_{xz}/d_{yz} displayed with turquoise diamonds. The lower inset shows one of the two components of the E_g (d_{xz}/d_{yz}) solution. (d,e) Leading gap structures of the Hund's coupling pairing scenario with $J/U = 0.5$. Note that these Hund's pair states correspond to dominant inter-orbital singlet, spin-triplet pairs [14, 15]. In (d) the usual convention for denoting the Fermi surface pockets is indicated. The colorbar shown in this plot is common for all gap plots.

the E_g solution can be stabilized when the k-SOC terms exhibit $\sin k_x \sin k_z$ or $\sin k_y \sin k_z$ structure, as was demonstrated recently in the case of Sr_2RuO_4 [6, 15, 23]. In contrast to the "Hund's coupling pairing scenario" based on constant attractive interactions, spin-fluctuation mediated pairing provides a route to superconductivity irrespective of the strength of SOC and Hund's coupling. In this mechanism, attractive channels are promoted by nesting features of the Fermi surface pockets, enabling a number of near-degenerate superconducting instabilities. These solutions belong to different irreducible representations of the D_{4h} point group and have highlighted the concept of accidental degeneracies in the case of Sr_2RuO_4 [7, 31–36].

The above developments call for a closer comparison of the Hund's coupling versus spin-fluctuation-mediated pairing mechanisms for realistic 3D models for Sr_2RuO_4 . In Ref. 37 we have performed a direct comparison between these two mechanisms for different generic 2D band structures. Here for Sr_2RuO_4 , we are concerned with the question of how the leading gap solutions compare in terms of their momentum structure and critical temperature T_c . In addition, in the Hund's coupling pairing scenario, k-SOC terms are important for the resulting gap structure [15, 23], but how do such k-SOC terms alter the spin-fluctuation generated gaps? In fact, the close competition between different pairing symmetries in Sr_2RuO_4 [7, 32, 35, 38] makes it important to determine if such rather small changes in the underlying electronic structure can rearrange the hierarchy of superconducting

solutions. Therefore, regardless of the smallness of additional interplanar hybridization and k-SOC terms that are allowed in 3D models, such terms might affect the superconducting gap symmetry.

In this paper, we determine the leading superconducting instabilities from a 3D realistic band structure relevant for Sr_2RuO_4 . Our calculations reveal the effect of Hund's coupling on the leading gap structures in a broad parameter range and thereby connect the pairing outcomes from the spin-fluctuation mediated mechanism with the regime where onsite Hund's coupling enables superconducting pairing, which is $J/U > \frac{1}{3}$ at the mean-field level. Figure 1 provides an overview of the resulting evolution of the dominant instabilities as a function of J/U . The two different mechanisms agree on the overall symmetry of the gap solutions, favoring $A_{1g}(s')$ and $B_{1g}(d_{x^2-y^2})$ superconductivity. However, as seen from Fig. 1, the nodal structures of the superconducting gaps are very different, with additional nesting-enforced vertical line nodes present when superconductivity is generated by spin fluctuations, see Fig. 1(a,b). Furthermore, a comparison of the leading eigenvalues of the two different mechanisms displayed in Fig. 1(c) highlights the fact that the eigenvalues, and hence T_c , for the Hund's pairing mechanism are much smaller compared to the spin-fluctuation mechanism. This appears to indicate that this version of Hund's coupling pairing may not be directly applicable to a correlated material like Sr_2RuO_4 , which exhibits significant momentum structure in its magnetic susceptibility. Finally, we remark

that longer-range Coulomb repulsion promote d_{xy} pairing, as shown recently within 2D models [7]. Therefore, due to the relatively weak 3D effects in Sr_2RuO_4 , we expect that many of the results shown below remain valid when including longer-range Coulomb repulsion except $d_{x^2-y^2}$ gets replaced by d_{xy} , but we have not further explored such effects in the present paper.

Additionally, we compute the dynamical spin susceptibility in relevant superconducting states for 3D Sr_2RuO_4 . It is found that only $d_{x^2-y^2}$ and d_{xz}/d_{yz} superconductivity support neutron resonances, whereas for example $s' + id_{x^2-y^2}$ does not. Lastly, a calculation of the uniform susceptibility shows that both $s' + id_{x^2-y^2}$ and $d_{xz} + id_{yz}$ exhibit pronounced Knight shifts, even though the former structure appears more compatible with recent bounds on the residual susceptibility at the lowest temperatures [10]. We discuss these findings in light of known experimental measurements of these quantities.

II. MODEL AND METHOD

The presence of inversion and time-reversal symmetries in the normal state Hamiltonian allows for 15 distinct non-zero terms within the t_{2g} orbital subset [23, 39], which include spin-preserving hopping terms, hybridizations, as well as onsite and momentum-dependent SOC. The latter depends explicitly on spin and includes both spin-flipping and spin-preserving processes. The full normal state Hamiltonian takes the form of a 6×6 matrix

$$H_{\text{NS}} = \left(\begin{array}{c|c} H_0 + H_{\text{SOC}}^+ & H_{\text{hyb}} + H_{\text{SOC}}^{3D} \\ \hline (H_{\text{hyb}} + H_{\text{SOC}}^{3D})^\dagger & H_0 + H_{\text{SOC}}^- \end{array} \right), \quad (1)$$

in the pseudospin basis $[\Psi(\mathbf{k}, +), \Psi(\mathbf{k}, -)]$. Here, $\Psi(\mathbf{k}, \sigma) = [d_{\mathbf{k},xz,\sigma}, d_{\mathbf{k},yz,\sigma}, d_{\mathbf{k},xy,\bar{\sigma}}]$ and $d_{\mathbf{k},\mu,\sigma}$ denotes the annihilation of an electron in orbital μ and spin state σ with momentum \mathbf{k} .

In Eq. (1) the electronic dispersion of the three orbitals is given by

$$H_0(\mathbf{k}) = \begin{pmatrix} \xi_{xz}(\mathbf{k}) & g(\mathbf{k}) & 0 \\ g(\mathbf{k}) & \xi_{yz}(\mathbf{k}) & 0 \\ 0 & 0 & \xi_{xy}(\mathbf{k}) \end{pmatrix}, \quad (2)$$

with $\xi_{xz/yz}(\mathbf{k}) = -2t_{1/2} \cos k_x - 2t_{2/1} \cos k_y - \mu$, $\xi_{xy}(\mathbf{k}) = -2t_3(\cos k_x + \cos k_y) - 4t_4 \cos k_x \cos k_y - 2t_5(\cos 2k_x + \cos 2k_y) - \mu$, and a hybridization of the form $g(\mathbf{k}) = -4t' \sin(k_x) \sin(k_y) - 8t'' \sin(k_x/2) \sin(k_y/2) \cos(k_z/2)$. The onsite and momentum-dependent SOC terms enter-

ing in the block diagonals of Eq. (1) are given by

$$H_{\text{SOC}}^\sigma(\mathbf{k}) = \frac{1}{2} \begin{pmatrix} 0 & -i\sigma\lambda_{so} & i\lambda_{so} \\ i\sigma\lambda_{so} & 0 & -\sigma\lambda_{so} \\ -i\lambda_{so} & -\sigma\lambda_{so} & 0 \end{pmatrix} + \begin{pmatrix} 0 & 0 & \sigma\alpha_{\mathbf{k}} - i\beta_{\mathbf{k}} \\ 0 & 0 & -i\alpha_{\mathbf{k}} - \sigma\beta_{\mathbf{k}} \\ \sigma\alpha_{\mathbf{k}} + i\beta_{\mathbf{k}} & i\alpha_{\mathbf{k}} - \sigma\beta_{\mathbf{k}} & 0 \end{pmatrix}, \quad (3)$$

where λ_{so} denotes the atomic SOC ($\mathbf{L} \cdot \mathbf{S}$) and $\alpha_{\mathbf{k}}, \beta_{\mathbf{k}}$ are momentum-dependent, spin-flip SOC terms given by

$$\alpha_{\mathbf{k}} = 4t_{dxy} \sin(k_x) \sin(k_y), \quad (4)$$

$$\beta_{\mathbf{k}} = 2t_d(\cos(k_x) - \cos(k_y)). \quad (5)$$

These higher order coupling terms can arise from the presence of orbital hybridizations and atomic SOC [6]. Additional momentum-dependent SOC is given by the off-diagonal contributions to the normal state Hamiltonian

$$H_{\text{SOC}}^{3D}(\mathbf{k}) = \begin{pmatrix} 0 & \eta_{\mathbf{k}}^x - i\eta_{\mathbf{k}}^y & -i\gamma_{\mathbf{k}}^y \\ -\eta_{\mathbf{k}}^x + i\eta_{\mathbf{k}}^y & 0 & -i\gamma_{\mathbf{k}}^x \\ -i\gamma_{\mathbf{k}}^y & -i\gamma_{\mathbf{k}}^x & 0 \end{pmatrix}, \quad (6)$$

with

$$\eta_{\mathbf{k}}^x = 8t_{12z} f_x(\mathbf{k}), \quad \eta_{\mathbf{k}}^y = -8t_{12z} f_y(\mathbf{k}), \quad (7)$$

$$\gamma_{\mathbf{k}}^x = 8t_{56z} f_x(\mathbf{k}), \quad \gamma_{\mathbf{k}}^y = -8t_{56z} f_y(\mathbf{k}), \quad (8)$$

and form factors given by

$$f_x(\mathbf{k}) = \cos(k_x/2) \sin(k_y/2) \sin(k_z/2), \quad (9)$$

$$f_y(\mathbf{k}) = \sin(k_x/2) \cos(k_y/2) \sin(k_z/2). \quad (10)$$

The η -terms are spin-flip processes between the xz and yz orbitals, while the γ -terms quantify spin-preserving transitions between the xz/yz and xy orbitals [6, 23]. It was previously shown that the γ -terms can give rise to an E_g gap solution in the presence of local attractions arising from large Hund's couplings, as discussed in Refs. 6 and 23. In addition, the $\alpha_{\mathbf{k}}$ -terms of Eq. (4) can promote an $s + id_{xy}$ solution [6]. Since one of the goals of this study is to determine the viability of the E_g state, we will focus on the E_g -favorable k-SOC terms with momentum structure as detailed in Eqs. (9-10), i.e. finite values of t_{12z} and t_{56z} , and set $t_{dxy} = t_d = 0$.

Finally, in a 3D model, interplanar hybridizations between the xz/yz and xy orbitals are also allowed and enter the off-diagonal parts of Eq. (1). These additional terms are given by

$$H_{\text{hyb}}(\mathbf{k}) = \begin{pmatrix} 0 & 0 & T_{xz,xy}(\mathbf{k}) \\ 0 & 0 & T_{yz,xy}(\mathbf{k}) \\ T_{xz,xy}(\mathbf{k}) & T_{yz,xy}(\mathbf{k}) & 0 \end{pmatrix}, \quad (11)$$

with

$$T_{xz,xy}(\mathbf{k}) = -8t_{\text{int}} f_x(\mathbf{k}), \quad T_{yz,xy}(\mathbf{k}) = -8t_{\text{int}} f_y(\mathbf{k}). \quad (12)$$

TABLE I. Hopping parametrization with additional hybridizations in units of meV.

t_1	t_2	t_3	t_4	t_5	μ	t'	t''	t_{int}
88	9	80	40	5	109	3	-2.5	-2

With the above expressions for hybridization and k-SOC, we work in a Brillouin zone (BZ) given by $[-\pi, \pi] \times [-\pi, \pi] \times [-2\pi, 2\pi]$. We have introduced out-of-plane hybridization terms, t'' and t_{int} of similar amplitude as in Ref. 23 renormalized to the effective hopping parameters presented in Table I. We fix the onsite SOC to $\lambda_{so} = 35$ meV ($\simeq 0.4t_1$)[35] giving rise to a splitting of the bands along the zone diagonals in agreement with ARPES experiments [20]. The dependence of the pairing structure on the amplitude of λ_{so} has been explored in detail for 2D models in Ref. [35]. Also, we include finite values of hybridizations (see Table I) as well as k-SOC parametrized by $t_{12z} = 5$ meV and $t_{56z} = 3, 4$ meV. The interplanar k-SOC terms are chosen to be the maximum allowed values that provide a Fermi surface compatible with ARPES and introduce a significant three-dimensional spin structure (see Fig. 3). Setting all 3D couplings to zero, the band structure reduces to the 2D model investigated in Refs. 7, 35, and 36.

The bare multi-orbital interaction Hamiltonian is given by

$$\begin{aligned} \hat{H}_{\text{int}} = & U \sum_{i,\mu} n_{i\mu\uparrow} n_{i\mu\downarrow} + \frac{U'}{2} \sum_{i,\nu \neq \mu, \sigma} n_{i\mu\sigma} n_{i\nu\bar{\sigma}} \\ & + \frac{U' - J}{2} \sum_{i,\nu \neq \mu, \sigma} n_{i\mu\sigma} n_{i\nu\sigma} \\ & + \frac{J}{2} \sum_{i,\nu \neq \mu, \sigma} d_{i\mu\sigma}^\dagger d_{i\nu\bar{\sigma}}^\dagger d_{i\mu\bar{\sigma}} d_{i\nu\sigma} \\ & + \frac{J'}{2} \sum_{i,\nu \neq \mu, \sigma} d_{i\mu\sigma}^\dagger d_{i\mu\bar{\sigma}}^\dagger d_{i\nu\bar{\sigma}} d_{i\nu\sigma}, \end{aligned} \quad (13)$$

where i is a site index, μ, ν are orbital indices and $\sigma = -\bar{\sigma}$ refers to electronic spin. As usual, intra- and interorbital Coulomb scattering as well as Hund's coupling and pair-hopping terms are included, and $U' = U - 2J$, $J' = J$. [40] We rewrite the interaction Hamiltonian in the compact form

$$\hat{H}_{\text{int}} = \frac{1}{2} \sum_{\mathbf{k}, \mathbf{k}' \{\tilde{\mu}\}} [V(\mathbf{k}, \mathbf{k}')]_{\tilde{\mu}_3, \tilde{\mu}_4}^{\tilde{\mu}_1, \tilde{\mu}_2} d_{\mathbf{k}\tilde{\mu}_1}^\dagger d_{-\mathbf{k}\tilde{\mu}_3}^\dagger d_{-\mathbf{k}'\tilde{\mu}_2} d_{\mathbf{k}'\tilde{\mu}_4} \quad (14)$$

with $\tilde{\mu} = (\mu, \sigma)$ introduced as a joint index of orbital and electronic spin. The bare electron-electron interaction matrix is specified by

$$\begin{aligned} [U]_{\mu\bar{\sigma}\mu\sigma}^{\mu\sigma\mu\bar{\sigma}} &= U, & [U]_{\mu\bar{\sigma}\nu\sigma}^{\nu\sigma\mu\bar{\sigma}} &= U', & [U]_{\mu\bar{\sigma}\nu\sigma}^{\mu\sigma\nu\bar{\sigma}} &= J', \\ [U]_{\nu\bar{\sigma}\nu\sigma}^{\mu\sigma\mu\bar{\sigma}} &= J, & [U]_{\nu\sigma\mu\sigma}^{\mu\sigma\nu\sigma} &= U' - J, \end{aligned} \quad (15)$$

where μ and ν denote different orbitals.

Within the usual mean-field Hund's coupling pairing scheme, where onsite interactions mediate superconductivity, the effective interaction of Eq. (14) is given simply by the onsite interaction elements of Eq. (15). The attractive channel obtained for $J > U'$ generates spin-triplet, orbital-singlet superconducting order. In order to obtain a superconducting instability, however, a sizable SOC is required, since this will mix the off-Fermi level gap of spin-triplet orbital-singlet form with an intraband spin-singlet gap at the Fermi surface [14, 27, 30, 37, 41]. Here, we explore a range of different Hund's couplings $J/U = 0.1 - 0.5$, noting however that in the case of Sr_2RuO_4 the estimated value from constrained random phase approximation (RPA) calculations is $J/U \simeq 0.1 - 0.2$ [42–44].

In the spin-fluctuation mediated pairing mechanism, the effective interaction is derived from RPA diagrams in the normal state including onsite as well as momentum-dependent SOC. The complete pairing obtained in this framework is given by an expression resembling a multi-orbital RPA susceptibility in which the bare interactions have the multi-orbital matrix structure detailed in Eq. (15) [35, 45, 46]. The pairing kernel takes the well-known form [35]

$$\begin{aligned} [V(\mathbf{k}, \mathbf{k}')]_{\tilde{\mu}_3, \tilde{\mu}_4}^{\tilde{\mu}_1, \tilde{\mu}_2} = & [U]_{\tilde{\mu}_3, \tilde{\mu}_4}^{\tilde{\mu}_1, \tilde{\mu}_2} + \left[U \frac{1}{1 - \chi_0 U} \chi_0 U \right]_{\tilde{\mu}_3, \tilde{\mu}_4}^{\tilde{\mu}_1, \tilde{\mu}_2}(\mathbf{k} + \mathbf{k}') \\ & - \left[U \frac{1}{1 - \chi_0 U} \chi_0 U \right]_{\tilde{\mu}_3, \tilde{\mu}_2}^{\tilde{\mu}_1, \tilde{\mu}_4}(\mathbf{k} - \mathbf{k}'), \end{aligned} \quad (16)$$

and includes the local bare interactions as well as explicit momentum-dependent effective interactions originating from higher-order processes mediated by the multiorbital susceptibility χ_0 . Nesting features of the Fermi surface are important for the pairing structure arising within this mechanism.

We parametrize the Fermi surface by roughly 3000 k-points and calculate the superconducting instabilities at the Fermi surface from the linearized gap equation

$$-\frac{1}{(2\pi)^3} \int_{FS} d\mathbf{k}'_f \frac{1}{v(\mathbf{k}'_f)} \Gamma_{l,l'}(\mathbf{k}_f, \mathbf{k}'_f) \Delta_{l'}(\mathbf{k}'_f) = \lambda \Delta_l(\mathbf{k}_f), \quad (17)$$

where $\Gamma_{l,l'}(\mathbf{k}_f, \mathbf{k}'_f)$ denotes the pairing kernel projected to band- and pseudospin-space [35], and \mathbf{k}_f denote the wave vectors on the Fermi surface. The Fermi speed is given by $v(\mathbf{k}_f)$. The leading superconducting instability is given by the gap function $\Delta_l(\mathbf{k}_f)$ with the largest eigenvalue λ and $T_c \propto e^{-1/\lambda}$. The pseudospin classification is encoded in the subscripts $l, l' = 0, x, y, z$ which refer to the components of the $\mathbf{d}(\mathbf{k})$ -vector in pseudospin space [47]. Even parity solutions appear in the $l = 0$, pseudospin singlet channel.

III. RESULTS

A. Gap structure

As seen from Fig. 1, the leading and subleading instabilities appear in the s' and $d_{x^2-y^2}$ channels. This result is very robust to parameter variations. In the present case, it is obtained for the band parametrization stated in Table I, setting $\lambda_{so} = 35$ meV, $t_{12z} = 5$ meV and $t_{56z} = 3$ meV. The susceptibility entering the pairing kernel in Eq. (16) is calculated at $k_B T = 2$ meV. The same two leading gap solutions arise both in the case when pairing is mediated by spin fluctuations, Eq.(16), and when it is generated directly from onsite attractions (i.e. including only the first momentum-independent part of Eq.(16)) in the case $U' - J < 0$. The latter Hund's coupling mechanism requires additionally finite SOC [14, 27, 41]. Note, however, since $U' = U - 2J$ it makes little sense to go beyond $J/U = 0.5$ in the present situation. The detailed structure of the gaps at the Fermi surface is shown in Fig. 1(a,b) and Fig. 1(d,e) for both pairing mechanisms. Note the qualitatively distinct nodal structures supported by the two approaches. First, Fig. 1(a,b) show the solutions of the spin-fluctuation mechanism as formulated in Eq. (16). The leading s' solution from Fig. 1(a) features no symmetry-protected nodes, but displays a robust nodal structure which persists for the whole range of explored values of Hund's coupling. The nodal structure on the inner (β) pocket coincides with the accidental nodes of the subleading $d_{x^2-y^2}$ solution, see Fig. 1(b). This ensures a near-nodal structure on the inner (β) pocket of a composite order parameter of the form $\Delta_{A_{1g}} + e^{i\phi} \Delta_{B_{1g}}$ (and $\Delta_{A_{1g}} + e^{i\phi} \Delta_{B_{2g}}$), as discussed previously within 2D models for Sr_2RuO_4 [7, 35]. Second, as opposed to the involved nodal structure supported by the spin fluctuations, which is rooted in the changing orbital content at the Fermi surface [7], the Hund's pairing gap structures display only symmetry-dictated nodes. Thus, the leading A_{1g} solution is entirely nodeless as seen from Fig. 1(d), but does exhibit a non-trivial relative sign change between the inner (β) and two outer (α, γ) Fermi pockets [14]. Likewise, the B_{1g} solution features only its symmetry-dictated nodal structure, but also has an additional internal phase structure with a sign change of the simple $d_{x^2-y^2}$ form between the α, β and γ -pockets. As discussed previously, these Hund's pair states correspond to dominant inter-orbital singlet, spin-triplet pairs [14, 15]. The qualitatively distinct gap structures between the two mechanisms arise from significant contributions from the last two terms in Eq. (16). The bare interactions, first term in Eq. (16), contains the attractive Hund's pair hopping term, *also* within spin-fluctuation mechanism when $J/U > 1/3$, but for the present Sr_2RuO_4 band structure this direct attractive channel is simply overwhelmed by the higher-order processes, even at $J/U = 0.4 - 0.5$. Clearly, this result depends on the combined significance of interactions and the spin susceptibility supported by the under-

lying band structure. The competition/cooperation between spin-fluctuation generated solution versus Hund's pairing superconductivity is further explored in Ref. 37.

As evident from Fig. 1(c), the two-component E_g solution is suppressed in the spin-fluctuation pairing scenario with several additional 1D even-parity solutions preceding in the hierarchy of superconducting instabilities (not shown in Fig. 1) [24]. In the Hund's coupling pairing scheme on the other hand, it is the third leading instability, appearing right below the s and $d_{x^2-y^2}$ solutions. The Hund's pairing scenario can support a leading E_g solution, as discussed further below, but only in the unusual case where the onsite SOC is weaker compared to the k-SOC [23]. For the current band parametrization with an onsite SOC of $\lambda_{so} = 35$ meV and k-SOC terms of magnitude $t_{12z} = 5$ meV and $t_{56z} = 3$ meV, the gap structure of one of the two components of the E_g solution is shown in the inset in the bottom of Fig. 1(c). That gap structure is surprisingly similar within both pairing scenarios, i.e. the E_g solutions arising from spin fluctuations do not exhibit additional orbitally driven accidental nodes.

To further compare the two different pairing scenarios, we show in Fig. 1(c) the evolution of pairing eigenvalues as the Hund's coupling J/U increases. In the regime $J/U < 1/3$, the local (mean-field) Hund's pairing does not support superconductivity, since no attractive channels are activated. By contrast, spin-fluctuation mediated pairing generates attractive channels for all values of Hund's coupling. We find an increase of the eigenvalues with increasing J/U , but no crossover between the different symmetry channels. Note that for all Hund's exchange values J/U in Fig. 1(c), the eigenvalues of the spin-fluctuation pairing significantly dominate over the eigenvalues from the Hund's pairing scenario. In all regimes, we find that odd-parity, pseudo-spin triplet solutions are strongly suppressed. Lastly, we note that within spin-fluctuation-mediated pairing, the strength of the pairing depends on the proximity to the associated magnetic instability at U_c , i.e. U compared to the critical interaction strength which in the current case is $U_c \simeq 160$ meV for $J/U = 0.2$. Therefore, larger values of Coulomb repulsion cause a rapid increase in the eigenvalue (and hence T_c). This property is only relevant very close to the instability, however, which is not the generic parameter range explored in this paper.

The gap structures that we find for the spin-fluctuation pairing, Fig. 1(a,b), are reminiscent of the s' and $d_{x^2-y^2}$ gap structures reported previously in purely 2D calculations [7, 35, 48]. Compared to the 2D case, there are small differences in the gap structure resulting from the additional interplanar hybridization and k-SOC terms: the gap changes sign on the α pocket and a shift of the accidental node position towards the zone axes is present in the 3D gap structure. However, the detailed gap structure of Fig. 1(a,b) still exhibits a sign change of the gap for segments of the Fermi surface connected by the prominent nesting vector of the xz/yz orbitals,

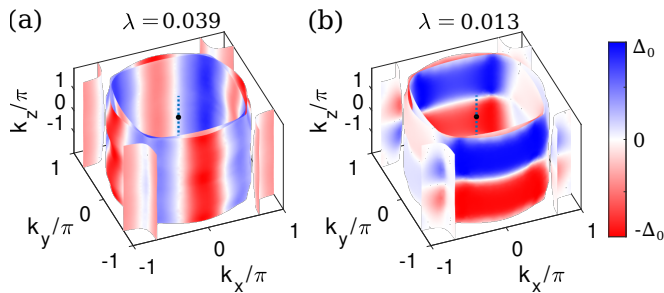


FIG. 2. (a) Leading $A_{1g}(s')$ gap structure arising within spin-fluctuation pairing for $U = 100$ meV and $J/U = 0.5$ for reduced onsite SOC $\lambda_{so} = 5$ meV and k-SOC $t_{56z} = 4$ meV. (b) Leading $E_g(d_{xz}/d_{yz})$ gap structure arising from Hund's coupling mediated pairing (one of the degenerate components shown) for the same parameters as in (a). The corresponding eigenvalue of the linearized gap equation is displayed in each sub-figure.

namely $\mathbf{Q}_1 \simeq (2\pi/3, 2\pi/3, q_z)$.

The gap structures presented in Fig. 1(a,b) are robust to changes in onsite Coulomb repulsion U and Hund's couplings. This leads to the conclusion that, despite the non-trivial 3D structure of the spin susceptibility entering the pairing kernel, the dominant and leading subdominant superconducting instabilities remain s' and $d_{x^2-y^2}$, with a similar gap structure as the ones obtained in the 2D case [7, 35]. Due to the demanding numerical procedure, we have not included longer-range interactions in the pairing kernel in the 3D calculations. However, based on the robustness of the s' and $d_{x^2-y^2}$ solutions when expanding the model from 2D to 3D, we expect a similar conclusion to hold when introducing longer-range interactions, in which case spin fluctuations will most likely lead to a near-degeneracy of s' and d_{xy} pairing states [7].

The ratio between onsite SOC and k-SOC is decisive for the appearance of a leading E_g solution within the Hund's pairing mechanism, as explored in Ref. 23. In particular, in the regime where λ_{so} and t_{56z} are comparable, the E_g solution is favored when $U' - J < 0$. In order to investigate the spin-fluctuation mechanism in the same regime of $\lambda_{so} \simeq t_{56z}$, we show in Fig. 2 the leading solutions of the two mechanisms for the case of $\lambda_{so} = 5$ meV and $t_{56z} = 4$ meV. As expected, the E_g solution is found to be leading within Hund's pairing, in this case for $J/U = 0.5$ (Fig. 2(b)). On the other hand, spin fluctuations favor an s' solution for the same set of parameters, i.e. in the strong Hund's coupling regime setting $U = 100$ meV despite the large value of $J/U = 0.5$. The subleading solution is $d_{x^2-y^2}$ and this continues to be the case also for smaller values of Hund's coupling $J/U = 0.25$ (not shown). Notably, the spin fluctuations yield an eigenvalue which is a factor of three larger than in the Hund's pairing mechanism. Again this value depends on U compared to U_c , but it remains a fact that λ is significantly larger within the spin-fluctuation approach for a wide range of interaction strengths [37]. Thus, even in the case where parameters are such that E_g is leading

within Hund's pairing, the momentum-dependent parts of the pairing kernel Eq. (16) overwhelm the gap structure arising purely from the onsite terms. In addition, we have explored the band structure of Ref. 23 in the specific case of $\lambda_{so} = 20$ meV and $t_{56z} = 15$ meV and found that while pure onsite interactions in the regime $J/U = 0.5$ supports the $E_g : d_{xz}/d_{yz}$ solution, spin fluctuations give a $d_{x^2-y^2}$ and s' near-degeneracy also for this band parametrization with largely enhanced eigenvalues compared to Hund's pairing.

B. Spin-susceptibility: neutron resonance and NMR Knight shift

We turn now to a discussion of the properties of the spin susceptibility in the leading superconducting candidate states that currently appear relevant for Sr_2RuO_4 . We focus on the question of a neutron resonance and the temperature T dependence of the NMR Knight shift.

The low-energy magnetic excitation spectrum at the incommensurate vector $\mathbf{Q}_1 \simeq (2\pi/3, 2\pi/3, q_z)$ has been probed in a number of recent neutron scattering studies [49–51]. Naively it is expected that, whatever its (unconventional) superconducting ground state, Sr_2RuO_4 should exhibit a neutron spin resonance, i.e. an enhancement of spectral weight below the superconducting gap edge 2Δ at momenta that correspond to peaks in the spin susceptibility and which connect regions on the Fermi surface on which the superconducting gap changes sign. Such a feature has been observed in inelastic neutron scattering on the cuprates, iron-based superconductors, and heavy-fermion systems, among others [52]. Indeed, in Ref. 51 a weak resonance-like feature at finite out-of-plane momentum $q_z = 0.5$ r.l.u. was reported. However, this finding remains controversial as it has not been reproduced, see e.g. Ref. 50, where scattering wave vectors near \mathbf{Q}_1 were carefully probed. Additionally, none of the neutron scattering studies find strong evidence for a pronounced opening of a gap in the spin excitation spectrum. We believe that this is a key experimental touchstone that may help to identify the structure of the superconducting gap in Sr_2RuO_4 .

In order to address these recent inelastic neutron measurements, we investigate the energy dependence of the spin susceptibility at \mathbf{Q}_1 for two different q_z vectors, $q_z = 0$ and 2π (note that we have chosen the BZ $[-\pi, \pi] \times [-\pi, \pi] \times [-2\pi, 2\pi]$ and therefore $q_z = 2\pi$ corresponds to an experimental value of $q_z = 0.5$ r.l.u.). The calculated static $\omega = 0$ spin susceptibility in the normal state is shown in Fig. 3, where the effect of SOC is visible in the difference between in-plane and out-of-plane spin components. For earlier theoretical works on the normal state spin susceptibility, we refer to Refs. [35, 38, 53–59]. In the corresponding 2D model, we find a larger out-of-plane spin component at the dominant peak structure at \mathbf{Q}_1 [7, 35]. Notably, as a result of the new k-SOC couplings, this anisotropy feature is now small and inverted

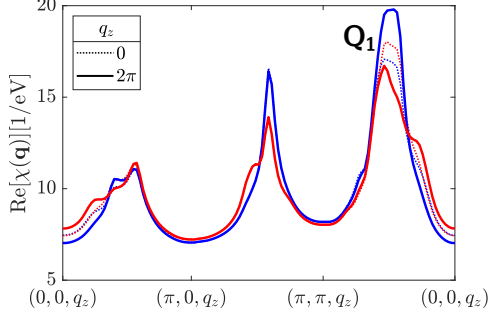


FIG. 3. Spin susceptibility of the normal state shown for a momentum path $(0, 0, q_z) \rightarrow (\pi, 0, q_z) \rightarrow (\pi, \pi, q_z) \rightarrow (0, 0, q_z)$ for $q_z = 0$ (dotted lines) and $q_z = 2\pi$ (full lines) for $U = 100$ meV and $J/U = 0.25$. The blue data shows the out-of-plane spin component, χ_{zz} , while red data displays the in-plane spin component, χ_{+-} .

at $q_z = 0$, but well-pronounced at $q_z = 2\pi$.

We address the possible gap structures proposed by spin-fluctuation mediated pairing, i.e. s' , $d_{x^2-y^2}$ (see Fig. 1(a,b)) and the combination $s' + id_{x^2-y^2}$ as well as the Hund's pairing proposed $d_{xz} + id_{yz}$ gap structure, of which one component is shown in Fig. 2(b). We approximate the RPA results for the different gap structures in terms of crystal harmonics. For example, for the s' gap we use

$$\Delta(k) = a + b(\cos k_x + \cos k_y) + c(\cos k_x \cos k_y), \quad (18)$$

with band-dependent values for the coefficients a , b and c . Similarly, the $d_{x^2-y^2}$ gap is parametrized in terms of $\cos k_x - \cos k_y$ and $\cos 2k_x - \cos 2k_y$. For these two gap structures, we neglect the k_z dependence, which we find to be negligible in our RPA results. The E_g gap is parametrized in terms of $\sin k_x$, $\sin k_y$, $\sin 2k_x$, $\sin 2k_y$, $\sin k_x \cos k_y$ and $\sin k_y \cos k_x$ crystal harmonics with an overall $\sin k_z/2$ form factor. We then include an additional Gaussian envelope of the form $\exp[-\epsilon_\nu(\mathbf{k})/\Omega_0]$ where $\epsilon_\nu(\mathbf{k})$ is the eigenenergy of band ν such that it cuts off the gap for momenta away from the Fermi surface. For all the parametrizations, we use coefficients that lead to a maximum gap size of approximately $\Delta_{\max} = 10$ meV. Numerical limitations prevent us from reducing the gap size further. This should not be a significant limitation, however, as the normal state density of states in our band structure is featureless over significantly larger energy scales.

The calculated low-energy spin susceptibility is shown in Fig. 4 for the different gap structures. As seen in the depiction in Figs. 1 and 2, the gap magnitudes vary considerably over the Fermi surface sheets. Due to this strong gap anisotropy, there is no clear opening of a well-defined spin-gap 2Δ , although there is a suppression of spectral weight at energies below 2Δ . At the same time, there is no clear spin resonance at \mathbf{Q}_1 for an interaction

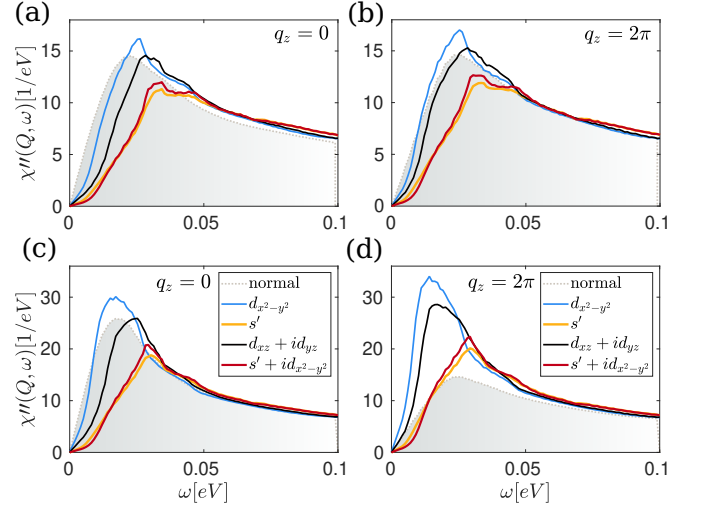


FIG. 4. Energy dependence of the imaginary part of the transverse spin susceptibility $\chi''(\mathbf{Q}_1, \omega)$ in the superconducting state for different gap symmetries $d_{x^2-y^2}$ (blue line), $E_g(d_{xz} + id_{yz})$ (black line), s' (orange line) and $s' + id_{x^2-y^2}$ (red line). The normal state spectra are depicted by the shaded area. The bare interaction parameters are (a,b) $U = 120$ meV $J/U = 0.25$, and (c,d) $U = 140$ meV $J/U = 0.25$.

strength $U = 120$ meV ($J/U = 0.25$), see Fig. 4(a,b). Nevertheless, for larger interactions ($U = 140$ meV) shown in Fig. 4(c,d), the spectral weight enhancement for the $d_{x^2-y^2}$ gap moves down to lower frequencies below 2Δ and gets significantly stronger for both $q_z = 0$ and $q_z = 2\pi$, indicating that this is indeed a resonance-like feature. Also, the two-component $d_{xz} + id_{yz}$ solution displays a broad resonance feature for larger U , but exclusively in the case of $q_z = 2\pi$, see Fig. 4(d). This is expected since for scattering at \mathbf{Q}_1 , the gap only changes sign for $2\pi < q_z < 4\pi$, see Fig. 2(b). As mentioned above, in the recent study by Iida *et al.*, a neutron resonance-like feature was found at this q_z position [51]. This appears to be in line with our theoretical findings for $d_{xz} + id_{yz}$ superconductivity. We stress, however, that the resonance found at \mathbf{Q}_1 for $q_z = 0.5$ r.l.u. in Ref. 51 has not been confirmed by another detailed study of the out-of-plane momentum dependence of the spin fluctuations, see Ref. 50. Finally, as seen from Fig. 4, neither the s' nor the $s' + id_{x^2-y^2}$ solutions exhibit resonance features at any interaction strength or q_z values.

Lastly, we turn to a discussion of the Knight shift which is calculated as the real part of the spin susceptibility at zero momentum, $\chi(\mathbf{q} = 0, \omega = 0)$, as a function of T normalized to the normal state value $\chi_{\text{NS}}(\mathbf{q} = 0, \omega = 0)$. We consider two candidate superconducting gap structures, namely the $d_{xz} + id_{yz}$ state stabilized within Hund's pairing, and the $s' + id_{x^2-y^2}$ phase favored by spin-fluctuation mediated pairing. Both orders break time-reversal symmetry. The T -dependence of the gap is introduced explicitly by the BCS form $\Delta(T) = \Delta_0 \tanh\left(1.76\sqrt{\frac{T_c}{T}} - 1\right)$,

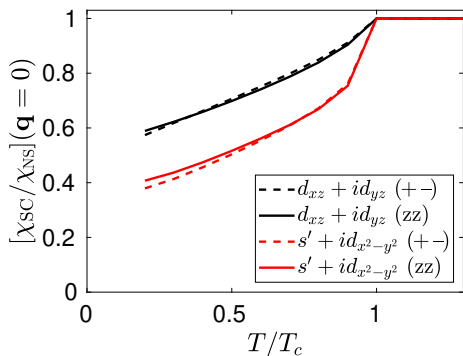


FIG. 5. Knight shift calculated as the ratio $\chi_{\text{SC}}(\mathbf{q} = 0)/\chi_{\text{NS}}(\mathbf{q} = 0)$ at zero energy as a function of temperature T for the two (time-reversal symmetry broken) gap structures $d_{xz} + id_{yz}$ (black curves) and $s' + id_{x^2-y^2}$ (red curves) for $U = 140$ meV and $J/U = 0.25$. The in-plane (out-of-plane) spin susceptibility is shown by dashed (full) lines.

with $\Delta_0 = 1$ meV at the position of maximum gap magnitude and $T_c = 0.5$ meV. Both gap structures display a considerable suppression of the uniform spin susceptibility at the lowest T , as shown in Fig. 5. There is only a small difference between in-plane and out-of-plane susceptibility components. As seen from Fig. 5, the decrease is only partial, with the ratio $\nu = \chi(T \ll T_c)/\chi(T > T_c) \simeq 0.4$ for the $s' + id_{x^2-y^2}$ gap, and $\nu \simeq 0.6$ for the $d_{xz} + id_{yz}$ gap. Importantly, the recent NMR experiment by Chronister *et al.*[10] proposes an upper bound of the condensate response to be less than 10 % of the normal state value. As seen from Fig. 5 both time-reversal symmetry broken states violate the "Chronister bound". We have not further explored quantitative match with this here. However, as discussed in Ref. 7 for the case of $s' + id_{xy}$ superconductivity, the magnitude of ν depends rather sensitively on the amplitude of SOC and interaction parameters U and J . Based on these calculations, it appears hard to reconcile a sizable SOC with $\nu < 10$ %.

IV. DISCUSSION AND CONCLUSIONS

Even though the $E_u : p_x/p_y$ spin-triplet order appears ruled out by recent Knight shift measurements [8, 9], several other experiments require certain combinations of two superconducting components [2, 3, 60, 61]. By contrast, specific heat data under uniaxial pressure appears difficult to reconcile with a two-component homogeneous order parameter scenario [5, 62, 63]. Here, we have determined the microscopic nature of superconductivity from spin-fluctuations and Hund's pairing within 3D models for Sr_2RuO_4 . We find that s' - and d -wave even-parity solutions are robust leading superconducting states, similar to the findings from 2D models for this material. This points to the nodal $s' + id$ phase as a prominent candidate for reconciling many experiments. The $E_g : d_{xz}/d_{yz}$ even-parity order is not favored from

spin-fluctuations, even inside the Hund's pairing regime at large J/U . In addition, we note that the $d + ig$ state suggested on phenomenological grounds [4] also does not appear to be competitive within the current framework.

Hund's pairing as defined in this paper can be viewed as an approximation to spin-fluctuation pairing in the sense that the Hund's pairing kernel is simply the spin-fluctuation kernel without the momentum-dependent terms, see Eq. (16). From this perspective, the present finding is that even for $J > U'$ the momentum-dependent terms dominate for an electronic band structure and interaction strengths relevant for Sr_2RuO_4 , i.e. they produce significantly larger T_c and can lead to qualitatively different gap structures. Of course both spin-fluctuation pairing and (mean-field) Hund's pairing are approximate methods to solve the full many-body pairing problem, and it remains to be seen how the superconducting states generated by these respective mechanisms compare to other methods relevant for modelling the superconducting gap structure of Sr_2RuO_4 . For recent work along these lines, see e.g. Refs. 64–66. These works take a large-scale numerical approach to calculation of the post-RPA pairing vertex, predicting different interesting leading even- and odd-frequency pairing states. Thus far they are restricted to high energies, and it is presently unclear how they are related to the low-energy Hamiltonian relevant for a 1K superconductor.

Finally, we computed the spin susceptibility in the superconducting state of leading candidates for Sr_2RuO_4 . In contrast to the s' and $s' + id_{x^2-y^2}$ states, it is found that $d_{x^2-y^2}$ and $d_{xz} + id_{yz}$ orders support a sub- 2Δ neutron resonance, which appears in contradiction to the most comprehensive currently-available neutron scattering data [50]. In terms of the uniform susceptibility, both time-reversal symmetry broken states, $s' + id_{x^2-y^2}$ and $d_{xz} + id_{yz}$, exhibit significant Knight shifts at the lowest T , with the former appearing more compatible with recent bounds on the SOC-generated spin-triplet component [10]. Thus, in summary, the mystery of superconducting pairing in Sr_2RuO_4 remains a challenge, but from the perspective of spin-fluctuation mediated pairing the accidental $s' + id_{x^2-y^2}$ (or $s' + id_{xy}$ when including longer-range Coulomb interactions) state currently remains the favored superconducting order, and seems compatible with most experiments.

V. ACKNOWLEDGEMENTS

We thank O. Gingras, M. Roig and H. Røising for insightful conversations. A. T. R. and B. M. A. acknowledge support from the Independent Research Fund Denmark Grant No. 8021-00047B. T. A. M. was supported by the U.S. Department of Energy, Office of Basic Energy Sciences, Materials Sciences and Engineering Division. P. J. H. was supported by the U.S. Department of Energy under Grant No. DE-FG02-05ER46236.

-
- [1] Andrew P. Mackenzie, Thomas Scaffidi, Clifford W. Hicks, and Yoshiteru Maeno, “Even odder after twenty-three years: the superconducting order parameter puzzle of Sr_2RuO_4 ,” *npj Quantum Materials* **2**, 40 (2017).
- [2] Sayak Ghosh, Arkady Shekhter, F. Jerzembeck, N. Kikugawa, Dmitry A. Sokolov, Manuel Brando, A. P. Mackenzie, Clifford W. Hicks, and B. J. Ramshaw, “Thermodynamic evidence for a two-component superconducting order parameter in Sr_2RuO_4 ,” *Nature Physics* (2020).
- [3] S. Benhabib, C. Lupien, I. Paul, L. Berges, M. Dion, M. Nardone, A. Zitouni, Z. Q. Mao, Y. Maeno, A. Georges, L. Taillefer, and C. Proust, “Ultrasound evidence for a two-component superconducting order parameter in Sr_2RuO_4 ,” *Nature Physics* (2020).
- [4] Steven Allan Kivelson, Andrew Chang Yuan, Brad Ramshaw, and Ronny Thomale, “A proposal for reconciling diverse experiments on the superconducting state in Sr_2RuO_4 ,” *npj Quantum Materials* **5**, 43 (2020).
- [5] Roland Willa, Matthias Hecker, Rafael M. Fernandes, and Jörg Schmalian, “Inhomogeneous time-reversal symmetry breaking in Sr_2RuO_4 ,” *Phys. Rev. B* **104**, 024511 (2021).
- [6] Jonathan Clepkens, Austin W. Lindquist, and Hae-Young Kee, “Shadowed triplet pairings in Hund’s metals with spin-orbit coupling,” *Phys. Rev. Research* **3**, 013001 (2021).
- [7] Astrid T. Rømer, P. J. Hirschfeld, and Brian M. Andersen, “Superconducting state of Sr_2RuO_4 in the presence of longer-range Coulomb interactions,” *Phys. Rev. B* **104**, 064507 (2021).
- [8] A. Pustogow, Yongkang Luo, A. Chronister, Y.-S. Su, D. A. Sokolov, F. Jerzembeck, A. P. Mackenzie, C. W. Hicks, N. Kikugawa, S. Raghu, E. D. Bauer, and S. E. Brown, “Constraints on the superconducting order parameter in Sr_2RuO_4 from oxygen-17 nuclear magnetic resonance,” *Nature* **574**, 72–75 (2019).
- [9] Kenji Ishida, Masahiro Manago, Katsuki Kinjo, and Yoshiteru Maeno, “Reduction of the ^{17}O Knight Shift in the Superconducting State and the Heat-up Effect by NMR Pulses on Sr_2RuO_4 ,” *Journal of the Physical Society of Japan* **89**, 034712 (2020).
- [10] Aaron Chronister, Andrej Pustogow, Naoki Kikugawa, Dmitry A. Sokolov, Fabian Jerzembeck, Clifford W. Hicks, Andrew P. Mackenzie, Eric D. Bauer, and Stuart E. Brown, “Evidence for even parity unconventional superconductivity in Sr_2RuO_4 ,” *Proceedings of the National Academy of Sciences* **118**, e2025313118 (2021).
- [11] G. M. Luke, Y. Fudamoto, K. M. Kojima, M. I. Larkin, J. Merrin, B. Nachumi, Y. J. Uemura, Y. Maeno, Z. Q. Mao, Y. Mori, H. Nakamura, and M. Sigrist, “Time-reversal symmetry-breaking superconductivity in Sr_2RuO_4 ,” *Nature* **394**, 558–561 (1998).
- [12] Vadim Grinenko, Debarchan Das, Ritu Gupta, Bastian Zinkl, Naoki Kikugawa, Yoshiteru Maeno, Clifford W. Hicks, Hans-Henning Klauss, Manfred Sigrist, and Rustem Khasanov, “Unsplit superconducting and time reversal symmetry breaking transitions in Sr_2RuO_4 under hydrostatic pressure and disorder,” *Nature Communications* **12**, 3920 (2021).
- [13] E. Hassinger, P. Bourgeois-Hope, H. Taniguchi, S. René de Cotret, G. Grissonnanche, M. S. Anwar, Y. Maeno, N. Doiron-Leyraud, and Louis Taillefer, “Vertical line nodes in the superconducting gap structure of Sr_2RuO_4 ,” *Phys. Rev. X* **7**, 011032 (2017).
- [14] Oskar Vafek and Andrey V. Chubukov, “Hund interaction, spin-orbit coupling, and the mechanism of superconductivity in strongly hole-doped iron pnictides,” *Phys. Rev. Lett.* **118**, 087003 (2017).
- [15] Jonathan Clepkens, Austin W. Lindquist, Xiaoyu Liu, and Hae-Young Kee, “Higher angular momentum pairings in interorbital shadowed-triplet superconductors: Application to Sr_2RuO_4 ,” *Phys. Rev. B* **104**, 104512 (2021).
- [16] Y. Maeno, H. Hashimoto, K. Yoshida, S. Nishizaki, T. Fujita, J. G. Bednorz, and F. Lichtenberg, “Superconductivity in a layered perovskite without copper,” *Nature* **372**, 532–534 (1994).
- [17] C. Bergemann, A. P. Mackenzie, S. R. Julian, D. Forsythe, and E. Ohmichi, “Quasi-two-dimensional fermi liquid properties of the unconventional superconductor Sr_2RuO_4 ,” *Advances in Physics* **52**, 639–725 (2003).
- [18] A. Damascelli, D. H. Lu, K. M. Shen, N. P. Armitage, F. Ronning, D. L. Feng, C. Kim, Z.-X. Shen, T. Kimura, Y. Tokura, Z. Q. Mao, and Y. Maeno, “Fermi surface, surface states, and surface reconstruction in Sr_2RuO_4 ,” *Phys. Rev. Lett.* **85**, 5194–5197 (2000).
- [19] M. W. Haverkort, I. S. Elfimov, L. H. Tjeng, G. A. Sawatzky, and A. Damascelli, “Strong spin-orbit coupling effects on the fermi surface of Sr_2RuO_4 and Sr_2RhO_4 ,” *Phys. Rev. Lett.* **101**, 026406 (2008).
- [20] V.B. Zabolotnyy, D.V. Evtushinsky, A.A. Kordyuk, T.K. Kim, E. Carleschi, B.P. Doyle, R. Fittipaldi, M. Cuoco, A. Vecchione, and S.V. Borisenko, “Renormalized band structure of Sr_2RuO_4 : A quasiparticle tight-binding approach,” *Journal of Electron Spectroscopy and Related Phenomena* **191**, 48 – 53 (2013).
- [21] C. N. Veenstra, Z.-H. Zhu, M. Raichle, B. M. Ludbrook, A. Nicolaou, B. Slomski, G. Landolt, S. Kittaka, Y. Maeno, J. H. Dil, I. S. Elfimov, M. W. Haverkort, and A. Damascelli, “Spin-orbital entanglement and the breakdown of singlets and triplets in Sr_2RuO_4 revealed by spin- and angle-resolved photoemission spectroscopy,” *Phys. Rev. Lett.* **112**, 127002 (2014).
- [22] Yuri Fukaya, Tatsuki Hashimoto, Masatoshi Sato, Yukio Tanaka, and Keiji Yada, “Spin susceptibility for orbital-singlet Cooper pair in the three-dimensional Sr_2RuO_4 superconductor,” *Phys. Rev. Research* **4**, 013135 (2022).
- [23] Han Gyeol Suh, Henri Menke, P. M. R. Brydon, Carsten Timm, Aline Ramires, and Daniel F. Agterberg, “Stabilizing even-parity chiral superconductivity in Sr_2RuO_4 ,” *Phys. Rev. Research* **2**, 032023 (2020).
- [24] Henrik S. Røising, Thomas Scaffidi, Felix Flicker, Gunnar F. Lange, and Steven H. Simon, “Superconducting order of Sr_2RuO_4 from a three-dimensional microscopic model,” *Phys. Rev. Research* **1**, 033108 (2019).
- [25] Wen Huang and Hong Yao, “Possible three-dimensional nematic odd-parity superconductivity in Sr_2RuO_4 ,” *Phys. Rev. Lett.* **121**, 157002 (2018).
- [26] Fabian Jerzembeck, Henrik S. Røising, Alexander Steppke, Helge Rosner, Dmitry A. Sokolov, Naoki Kikugawa, Thomas Scaffidi, Steven H. Simon, Andrew P.

- Mackenzie, and Clifford W. Hicks, “The Superconductivity of Sr_2RuO_4 Under c -Axis Uniaxial Stress,” arXiv e-prints, arXiv:2111.06228 (2021), arXiv:2111.06228 [cond-mat.supr-con].
- [27] Christoph M. Puetter and Hae-Young Kee, “Identifying spin-triplet pairing in spin-orbit coupled multi-band superconductors,” EPL (Europhysics Letters) **98**, 27010 (2012).
- [28] Yue Yu, Alfred K. C. Cheung, S. Raghu, and D. F. Agterberg, “Residual spin susceptibility in the spin-triplet orbital-singlet model,” Phys. Rev. B **98**, 184507 (2018).
- [29] R. Gupta, S. Shallcross, J. Quintanilla, M. Gradhand, and J. Annett, “Distinguishing $d_{xz} + id_{yz}$ and $d_{x^2-y^2}$ pairing in Sr_2RuO_4 by high magnetic field H–T phase diagrams,” (2021), arXiv:2111.00257 [cond-mat.supr-con].
- [30] Alfred K. C. Cheung and D. F. Agterberg, “Superconductivity in the presence of spin-orbit interactions stabilized by Hund coupling,” Phys. Rev. B **99**, 024516 (2019).
- [31] M. Eschrig, J. Ferrer, and M. Fogelström, “Mixed-parity superconductivity in Sr_2RuO_4 ,” Phys. Rev. B **63**, 220509 (2001).
- [32] Thomas Scaffidi, Jesper C. Romers, and Steven H. Simon, “Pairing symmetry and dominant band in Sr_2RuO_4 ,” Phys. Rev. B **89**, 220510(R) (2014).
- [33] Wan-Sheng Wang, Cong-Cong Zhang, Fu-Chun Zhang, and Qiang-Hua Wang, “Theory of chiral p -wave superconductivity with near nodes for Sr_2RuO_4 ,” Phys. Rev. Lett. **122**, 027002 (2019).
- [34] Zhiqiang Wang, Xin Wang, and Catherine Kallin, “Spin-orbit coupling and spin-triplet pairing symmetry in Sr_2RuO_4 ,” Phys. Rev. B **101**, 064507 (2020).
- [35] A. T. Rømer, D. D. Scherer, I. M. Eremin, P. J. Hirschfeld, and B. M. Andersen, “Knight shift and leading superconducting instability from spin fluctuations in Sr_2RuO_4 ,” Phys. Rev. Lett. **123**, 247001 (2019).
- [36] A. T. Rømer and B. M. Andersen, “Fluctuation-driven superconductivity in Sr_2RuO_4 from weak repulsive interactions,” Modern Physics Letters B **34**, 2040052 (2020).
- [37] Mercè Roig, Astrid T. Rømer, Andreas Kreisel, P. J. Hirschfeld, and Brian M. Andersen, “Superconductivity in multiorbital systems with repulsive interactions: Hund’s pairing vs. spin-fluctuation pairing,” preprint (2022).
- [38] O. Gingras, R. Nourafkan, A.-M. S. Tremblay, and M. Côté, “Superconducting Symmetries of Sr_2RuO_4 from First-Principles Electronic Structure,” Phys. Rev. Lett. **123**, 217005 (2019).
- [39] Aline Ramires and Manfred Sigrist, “Superconducting order parameter of Sr_2RuO_4 : A microscopic perspective,” Phys. Rev. B **100**, 104501 (2019).
- [40] Elbio Dagotto, Takashi Hotta, and Adriana Moreo, “Colossal magnetoresistant materials: the key role of phase separation,” Physics Reports **344**, 1–153 (2001).
- [41] Shintaro Hoshino and Philipp Werner, “Superconductivity from emerging magnetic moments,” Phys. Rev. Lett. **115**, 247001 (2015).
- [42] Jernej Mravlje, Markus Aichhorn, Takashi Miyake, Kristjan Haule, Gabriel Kotliar, and Antoine Georges, “Coherence-Incoherence Crossover and the Mass-Renormalization Puzzles in Sr_2RuO_4 ,” Phys. Rev. Lett. **106**, 096401 (2011).
- [43] Loïc Vaugier, Hong Jiang, and Silke Biermann, “Hubbard U and Hund exchange J in transition metal oxides: Screening versus localization trends from constrained random phase approximation,” Phys. Rev. B **86**, 165105 (2012).
- [44] A. Tamai, M. Zingl, E. Rozbicki, E. Cappelli, S. Riccò, A. de la Torre, S. McKeown Walker, F. Y. Bruno, P. D. C. King, W. Meevasana, M. Shi, M. Radović, N. C. Plumb, A. S. Gibbs, A. P. Mackenzie, C. Berthod, H. U. R. Strand, M. Kim, A. Georges, and F. Baumberger, “High-resolution photoemission on Sr_2RuO_4 reveals correlation-enhanced effective spin-orbit coupling and dominantly local self-energies,” Phys. Rev. X **9**, 021048 (2019).
- [45] A. T. Rømer, A. Kreisel, I. Eremin, M. A. Malakhov, T. A. Maier, P. J. Hirschfeld, and B. M. Andersen, “Pairing symmetry of the one-band Hubbard model in the paramagnetic weak-coupling limit: A numerical RPA study,” Phys. Rev. B **92**, 104505 (2015).
- [46] Astrid T. Rømer, Thomas A. Maier, Andreas Kreisel, Ilya Eremin, P. J. Hirschfeld, and Brian M. Andersen, “Pairing in the two-dimensional Hubbard model from weak to strong coupling,” Phys. Rev. Research **2**, 013108 (2020).
- [47] Manfred Sigrist and Kazuo Ueda, “Phenomenological theory of unconventional superconductivity,” Rev. Mod. Phys. **63**, 239–311 (1991).
- [48] Astrid T. Rømer, Andreas Kreisel, Marvin A. Müller, P. J. Hirschfeld, Ilya M. Eremin, and Brian M. Andersen, “Theory of strain-induced magnetic order and splitting of T_c and T_{trsb} in Sr_2RuO_4 ,” Phys. Rev. B **102**, 054506 (2020).
- [49] S. Kunkemöller, P. Steffens, P. Link, Y. Sidis, Z. Q. Mao, Y. Maeno, and M. Braden, “Absence of a large superconductivity-induced gap in magnetic fluctuations of Sr_2RuO_4 ,” Phys. Rev. Lett. **118**, 147002 (2017).
- [50] K. Jenni, S. Kunkemöller, P. Steffens, Y. Sidis, R. Bewley, Z. Q. Mao, Y. Maeno, and M. Braden, “Neutron scattering studies on spin fluctuations in Sr_2RuO_4 ,” Phys. Rev. B **103**, 104511 (2021).
- [51] Kazuki Iida, Maiko Kofu, Katsuhiko Suzuki, Naoki Murai, Seiko Ohira-Kawamura, Ryoichi Kajimoto, Yasuhiro Inamura, Motoyuki Ishikado, Shunsuke Hasegawa, Takatsugu Masuda, Yoshiyuki Yoshida, Kazuhisa Kakurai, Kazushige Machida, and Seunghun Lee, “Horizontal line nodes in Sr_2RuO_4 proved by spin resonance,” Journal of the Physical Society of Japan **89**, 053702 (2020).
- [52] D. J. Scalapino, “A common thread: The pairing interaction for unconventional superconductors,” Rev. Mod. Phys. **84**, 1383–1417 (2012).
- [53] Dirk K. Morr, Peter F. Trautman, and Matthias J. Graf, “Resonance peak in Sr_2RuO_4 : Signature of spin triplet pairing,” Phys. Rev. Lett. **86**, 5978–5981 (2001).
- [54] I. Eremin, D. Manske, and K.-H. Bennemann, “Electronic theory for the normal-state spin dynamics in Sr_2RuO_4 : Anisotropy due to spin-orbit coupling,” Phys. Rev. B **65**, 220502(R) (2002).
- [55] Masahisa Tsuchiizu, Youichi Yamakawa, Seiichiro Onari, Yusuke Ohno, and Hiroshi Kontani, “Spin-triplet superconductivity in Sr_2RuO_4 due to orbital and spin fluctuations: Analyses by two-dimensional renormalization group theory and self-consistent vertex-correction method,” Phys. Rev. B **91**, 155103 (2015).
- [56] Sergio Cobo, Felix Ahn, Ilya Eremin, and Alireza Akbari, “Anisotropic spin fluctuations in Sr_2RuO_4 : Role of spin-orbit coupling and induced strain,” Phys. Rev. B **94**, 224507 (2016).

- [57] Lewin Boehnke, Philipp Werner, and Frank Lechermann, “Multi-orbital nature of the spin fluctuations in Sr_2RuO_4 ,” *EPL (Europhysics Letters)* **122**, 57001 (2018).
- [58] Hugo U. R. Strand, Manuel Zingl, Nils Wentzell, Olivier Parcollet, and Antoine Georges, “Magnetic response of Sr_2RuO_4 : Quasi-local spin fluctuations due to Hund’s coupling,” *Phys. Rev. B* **100**, 125120 (2019).
- [59] Swagata Acharya, Dimitar Pashov, Cédric Weber, Hyowon Park, Lorenzo Sponza, and Mark Van Schilfgaarde, “Evening out the spin and charge parity to increase T_c in Sr_2RuO_4 ,” *Communications Physics* **2**, 163 (2019).
- [60] Jing Xia, Yoshiteru Maeno, Peter T. Beyersdorf, M. M. Fejer, and Aharon Kapitulnik, “High resolution polar kerr effect measurements of Sr_2RuO_4 : Evidence for broken time-reversal symmetry in the superconducting state,” *Phys. Rev. Lett.* **97**, 167002 (2006).
- [61] Vadim Grinenko, Shreenanda Ghosh, Rajib Sarkar, Jean-Christophe Orain, Artem Nikitin, Matthias Elender, Debarchan Das, Zurab Guguchia, Felix Brückner, Mark E. Barber, Joonbum Park, Naoki Kikugawa, Dmitry A. Sokolov, Jake S. Bobowski, Takuto Miyoshi, Yoshiteru Maeno, Andrew P. Mackenzie, Hubertus Luetkens, Clifford W. Hicks, and Hans-Henning Klauss, “Split superconducting and time-reversal symmetry-breaking transitions in Sr_2RuO_4 under stress,” *Nature Physics* **17**, 748–754 (2021).
- [62] You-Sheng Li, Naoki Kikugawa, Dmitry A. Sokolov, Fabian Jerzembeck, Alexandra S. Gibbs, Yoshiteru Maeno, Clifford W. Hicks, Jörg Schmalian, Michael Nicklas, and Andrew P. Mackenzie, “High-sensitivity heat-capacity measurements on Sr_2RuO_4 under uniaxial pressure,” *Proceedings of the National Academy of Sciences* **118**, e2020492118 (2021).
- [63] Glenn Wagner, Henrik S. Røising, Felix Flicker, and Steven H. Simon, “Microscopic ginzburg-landau theory and singlet ordering in Sr_2RuO_4 ,” *Phys. Rev. B* **104**, 134506 (2021).
- [64] Stefan Käser, Hugo U. R. Strand, Nils Wentzell, Antoine Georges, Olivier Parcollet, and Philipp Hansmann, “Inter-orbital singlet pairing in Sr_2RuO_4 : a Hund’s superconductor,” *arXiv e-prints*, arXiv:2105.08448 (2021), arXiv:2105.08448 [cond-mat.str-el].
- [65] Olivier Gingras, Nikita Allaglo, Reza Nourafkan, Michel Côté, and André-Marie S. Tremblay, “Frequency-dependent Inter-pseudospin Solutions to Superconducting Strontium Ruthenate,” *arXiv e-prints*, arXiv:2201.08917 (2022), arXiv:2201.08917 [cond-mat.supr-con].
- [66] Olivier Gingras, Nikita Allaglo, Reza Nourafkan, Michel Côté, and André-Marie S. Tremblay, “Coexistence of Even- and Odd-Frequency Superconductivity in Correlated Multi-Orbital Systems with Spin-Orbit Coupling,” *arXiv e-prints*, arXiv:2201.08918 (2022), arXiv:2201.08918 [cond-mat.supr-con].